Structures and Vibrational Frequencies of Vanadium (V) Oligomers: An *Ab Initio* Study Using Effective Core Potentials

PAULO J. A. RIBEIRO-CLARO,* ANA MARGARIDA AMADO, and J. J. C. TEIXEIRA-DIAS

Unidade I & D "Química-Física Molecular," Departamento de Química, Universidade de Coimbra, P-3049 Coimbra, Portugal

Received 30 July 1995; accepted 16 October 1995

ABSTRACT

Ab initio molecular geometries and vibrational frequencies of various isolated vanadate species (VO_4^{3-}, HVO_4^{2-}, $H_2VO_4^-$, and $V_2O_7^{4-}$) were calculated using different pseudopotentials. The relative merits of these were assessed by comparing the calculated molecular parameters with the corresponding values obtained from calculations at all-electron levels and, whenever available, from X-ray studies for the salts. The calculations were extended to higher oligomers ($V_3O_{10}^{5-}$, $V_4O_{13}^{6-}$, and $V_4O_{12}^{4-}$) using the pseudopotential whose basis functions are $(10s5p5d)/[2s1p1d]$ (55/5/5) on vanadium and $(4s4p)/[2s2p]$ (31/31) on oxygen, which yielded the best compromise between accuracy and computational effort. The results indicate a linear centrosymmetric geometry for the isolated $V_2O_7^{4-}$ anion. The higher oligomers have less than 180° V—O—V angles, except the noncyclic tetraoligomer which has a linear central V—O—V angle (180°). The cyclic $V_4O_{12}^{4-}$ species presents a planar structure with all the vanadium and bridging oxygen atoms in the same plane. This structure was already reported for the $[(CH_3)CNH_3][V_4O_{12}]$ salt. The results suggest a lower stability of the linear $V_4O_{13}^{6-}$ species, in agreement with previous reports.

Introduction

While vanadium is a trace element, toxic at high concentration levels, it is well known by its biological impact.[1-3] In particular, it has been demonstrated that vanadium salts display insulin-like activity and may be used in the treatment of diabetes.[3] Most of the biological importance of vanadium is associated with the +5 oxidation state (vanadate) and is due to a similarity between the vanadate and the phosphate

* Author to whom correspondence should be addressed.

CCC 0192-8651 / 96 / 101183-14

chemistries.[4] For instance, it has been suggested that vanadate species induce cardiovascular activity and hormonal action,[5] and there have been a number of reports concerning the influence of vanadate on the activity of various enzymes—inhibiting some while stimulating others.[6] This scattered activity arises from the fact that vanadate aqueous solutions consist of complex mixtures of different oligomers, and experimental evidence shows that each of the vanadate oligomers invoke different responses in biological systems. Due to this great impact on various biochemical systems,[6] vanadate and its oligomeric species have undoubtedly been one of the most pursued oxyanion systems in the last few decades.

While accurate *ab initio* studies of molecular structure have become nearly a routine, the number of reports concerning the application of *ab initio* molecular calculations on vanadate oligomers are extremely scarce. To the best of our knowledge, all-electron *ab initio* studies published in the literature are restricted to the fixed geometry approximation, either on the smallest species[7] or using powerful computers not available to typical research groups.[8] This limitation, common to the generality of calculations on transition metal compounds, results naturally from the dramatic increase of computational cost with the number of explicitly treated electrons.

A breakthrough to this situation arose with the development of effective core potentials (ECPs) methods. In fact, by replacing the chemically inert electrons of the core by a fixed potential, ECPs reduce the molecular calculation to a valence-electron problem, thus cutting considerably the computational costs. Some calculations on vanadate ions using this approximation have already been published.[9] However, the application of an ECP to molecular problems still suffers from a lack of systematic studies concerning its performance in reproducing experimental properties and calculated all-electron (AE) results on these systems.

The purpose of the present study is twofold. First, to compare the performance of different levels of ECP sophistication on small vanadate species, in order to choose the ECP which yields the best compromise between computational effort and consistency of values for this particular set of molecules. Second, to calculate the molecular geometries of species like $(HO)_4VO^-$, $V_2O_7^{4-}$, $V_3O_{10}^{5-}$, $V_4O_{13}^{6-}$, and $V_4O_{12}^{4-}$, considered to be important species in basic aqueous solution.[10,11]

Experimental

Calculations were performed using the Gaussian 92 program package[12] adapted to a Vax 9000-210 computer.

Table I presents the basis sets used in this work. In particular, various ECPs, with different core-valence partitioning and splittings schemes, tested for VO_4^{3-}, $(HO)VO_3^{2-}$, $(HO)_2VO_2^-$, and $V_2O_7^{4-}$ species, are shown there.

In order to evaluate the influence of the core-valence partitioning scheme on vanadium atom, two kinds of ECPs were tested: one which treats explicitly the $3d$ and $4s$ electrons[13] (HS1 to HS4); the other which also treats explicitly the outermost core orbitals ($3s$ and $3p$)[14] (HS5 to HS11). In addition, different splittings both on vanadium and oxygen were considered. On oxygen, the performance of minimal and double-zeta (DZ) basis sets[15] was tested, while splittings ranging from minimal to DZ2P[16] were used on vanadium. In addition, one ECP due to Christiansen et al.[17,18] was considered. Also, various tests were made by including in some of the previous ECPs a diffuse (flat) function ($\zeta = 0.0845$)[19] and/or a polarization function ($\zeta = 0.8$)[20] on oxygen.

The accuracy of the various ECPs was assessed by comparing their results with those from three AE basis sets. For oxygen and hydrogen, these basis sets used the same basis functions. In particular, for oxygen, all the basis sets correspond to the 3-21G[21] basis set with deliberately added d ($\zeta = 0.8$) and sp ($\zeta = 0.0845$) functions. For hydrogen, the AE basis sets include the 3-21G basis functions.[21] Hence, the AE basis sets used differ by their functions on the vanadium atoms, as follows:

AE1: STO-3G*.[12]

AE2: 3-21G.[22]

AE3: 3-21G supplemented with a d function ($\zeta = 0.39$).

For all these basis sets, the geometries of VO_4^{3-}, $(HO)VO_3^{2-}$, and $(HO)_2VO_2^-$ were fully optimized. In addition, the geometry of $V_2O_7^{4-}$ was fully optimized with AE1. The AE and ECP optimized geometries for VO_4^{3-}, $(HO)VO_3^{2-}$, $(HO)_2VO_2^-$, and $V_2O_7^{4-}$ were used for the calculation of vibrational frequencies at the same level. These were obtained by using analytic and numeric second derivatives at the AE and ECP levels, respectively. Atomic

TABLE I.
Basis Sets.[a]

Basis Functions on V	Basis Functions on O	Designation[b]
ECPs		
(3*s*2*p*5*d*) / [1*s*1*p*1*d*] (3 / 2 / 5)	(4*s*4*p*) / [1*s*1*p*] (4 / 4)	HS1
(3*s*2*p*5*d*) / [1*s*1*p*1*d*] (3 / 2 / 5)	(4*s*4*p*) / [2*s*2*p*] (31 / 31)	HS2
(3*s*2*p*5*d*) / [2*s*2*p*2*d*] (21 / 11 / 41)	(4*s*4*p*) / [2*s*2*p*] (31 / 31)	HS3
(3*s*2*p*5*d*) / [3*s*2*p*3*d*] (111 / 11 / 311)	(4*s*4*p*) / [2*s*2*p*] (31 / 31)	HS4
(10*s*5*p*5*d*) / [2*s*1*p*1*d*] (55 / 5 / 5)	(4*s*4*p*) / [1*s*1*p*] (4 / 4)	HS5
(9*s*5*p*5*d*) / [3*s*2*p*2*d*] (441 / 41 / 41)	(4*s*4*p*) / [1*s*1*p*] (4 / 4)	HS6
(9*s*5*p*5*d*) / [3*s*3*p*2*d*] (441 / 311 / 41)	(4*s*4*p*) / [1*s*1*p*] (4 / 4)	HS7
(10*s*5*p*5*d*) / [2*s*1*p*1*d*] (55 / 5 / 5)	(4*s*4*p*) / [2*s*2*p*] (31 / 31)	HS8
(9*s*5*p*5*d*) / [3*s*2*p*2*d*] (441 / 41 / 41)	(4*s*4*p*) / [2*s*2*p*] (31 / 31)	HS9
(9*s*5*p*5*d*) / [3*s*3*p*2*d*] (441 / 311 / 41)	(4*s*4*p*) / [2*s*2*p*] (31 / 31)	HS10
(9*s*5*p*5*d*) / [3*s*4*p*2*d*] (441 / 2111 / 41)	(4*s*4*p*) / [2*s*2*p*] (31 / 31)	HS11
(14*s*6*p*6*d*) / [2*s*1*p*1*d*] (77 / 6 / 6)	(4*s*4*p*) / [1*s*1*p*] (4 / 4)	CC1
AE		
STO-3G + *d* (ζ = 0.39)	3-21G + *d* (ζ = 0.8) + *sp* (ζ = 0.0845)	AE1
3-21G	3-21G + *d* (ζ = 0.8) + *sp* (ζ = 0.0845)	AE2
3-21G + *d* (ζ = 0.39)	3-21G + *d* (ζ = 0.8) + *sp* (ζ = 0.0845)	AE3

[a] For hydrogen the basis sets simply correspond to 3-21G.
[b] H, S, and C stand for Hay et al. (refs. 13 and 14), Stevens et al. (ref. 15), and Hurley et al. (ref. 17), respectively. Basis sets from ref. 13 were used in the first four HS basis sets (from HS1 to HS4); basis sets from ref. 14 were used in the remaining HS basis sets (from HS5 to HS11).

charges have been computed from Mulliken population analysis.[23] Aside from the basis set dependence, this analysis has intrinsic limitations resulting from the equipartition of the overlap density between atoms. Nevertheless, it is a computationally inexpensive and a widely used straightforward procedure.

Results and Discussion

MONOVANADATE SPECIES: VO_4^{3-} AND ITS PROTONATED FORMS

Table II shows the VO_4^{3-} molecular parameters (V—O bond lengths and atomic charges) obtained with the AE and ECP basis sets. Some experimental results[24,25] are also presented for comparison.

At the AE level, the V—O bond lengths are in good agreement with the experimental results, and the addition of a supplementary *d* function on the vanadium atom, in passing from AE2 to AE3, somewhat increases its positive charge, but does not affect the V—O bond length.

With regard to the ECP results, a vanadium core-valence partitioning scheme considering the 3*s* and 3*p* orbitals in the atom core (from HS1 to HS4) is definitively inappropriate for the geometry description of VO_4^{3-}, since these basis sets grossly overestimate the V—O bond length. This observation is in agreement with recent studies on several transition metal systems which show that the outermost core electrons must be treated explicitly and should not be replaced by an ECP.[26-29]

The overall agreement between the results of the remaining ECPs (from HS5 to HS11, and CC1; see Table II), which all include the vanadium 3*s* and 3*p* orbitals in the valence shell, with the AE and experimental results is quite good. In addition, the V—O bond length increases upon splitting of the oxygen valence shell. On the contrary, when a minimal basis is considered at the oxygen atoms, the splitting of the transition metal atom tends to diminish the V—O bond length (HS5 versus HS6 and HS7). In addition, no considerable effect is found on splitting the vanadium basis set (HS8 versus HS9, HS10, and HS11), provided the oxygen valence shell is split.

Table III presents the calculated vibrational frequencies for VO_4^{3-} with the AE and some of the ECP basis sets. In addition, some reported experimental values are also shown.

As can be seen, the AE frequencies are in reasonable agreement with the experimental values.

TABLE II.
***Ab Initio* Fully Optimized Molecular Parameters for VO_4^{3-} Species.**

	V—O (pm)	Charge/e[a] V	Charge/e[a] O
All-electron			
AE1	171	+2.9	−1.5
AE2	170	+1.9	−1.2
AE3	170	+2.1	−1.3
ECP			
HS1	236	−0.1	−0.7
HS2	228	+1.0	−1.0
HS3	225	+1.0	−1.0
HS4	225	+1.0	−1.0
HS5	172	+1.2	−1.1
HS6	168	+0.2	−0.8
HS7	169	−0.1	−0.7
HS8	173	+1.7	−1.2
HS9	172	+1.4	−1.1
HS10	172	+1.2	−1.1
HS11	173	+1.3	−1.1
CC1	170	+1.5	−1.1
Exp.			
b	171 ± 8		
c	171 ± 2		

[a] $e = 1.6021897 \times 10^{-19}$ C.
[b] Average value from Zn salt X-ray results (ref. 24).
[c] From ref. 25 and the observed ν V—O of ref. 11.

In what concerns the pseudopotential results, with the exception of HS1 and HS2, the generality of the ECPs yields reasonably accurate values.

In short, the above-mentioned observations show that the transition metal core-valence partitioning scheme is decisive for the evaluation of the molecular parameters of VO_4^{3-} (e.g., molecular geometry, vibrational frequencies, and atomic charges). A vanadium valence space composed only of the $3d$ and $4s$ electrons is definitely too small, and the inclusion of the $3s$ and $3p$ outermost vanadium core electrons is fundamental, even if the atom valence shell is triple-zeta split. The overall influence on the molecular geometry of splitting the oxygen and vanadium valence shells is quite small; it has the disadvantage of largely increasing the computational time. However, one should keep in mind that these conclusions are restricted to the particular kind of systems herein studied.

On proceeding to $(HO)VO_3^{2-}$, only the three ECPs which lead to the best compromise accuracy/computational cost for VO_4^{3-} species, i.e., HS5, HS8, and CC1, were considered. To the best of our knowledge, there are no experimental structural results concerning this species. Consequently, the performance of the ECP basis sets has to be judged by comparison with the AE results.

Table IV presents some molecular parameters (bond lengths, bond angles, and dihedral angles) obtained for $(HO)VO_3^{2-}$ with some of the ECPs, and compares them with the AE results. Figure 1a shows the minimum energy structure obtained for this vanadate species with the AE basis sets.

The calculated V—O bond lengths using the minimal ECPs (HS5, HS8, and CC1) are in good agreement with the AE results. What concerns the O_1—H bond length is that HS8 yields the most reasonable value; the remaining ECPs give somewhat longer values. On the other hand, the H—O—V and O—V—O bond angles are quite well reproduced by the three ECP basis sets.

The most controversial structural parameter is undoubtedly the $HO_1—VO_3$ dihedral angle. The AE calculations are unanimous in pointing to a eclipsed conformation as an energy minimum ($HO_1—VO_3 = 0°$; Fig. 1a). Among the minimal

TABLE III.
VO_4^{3-} Vibrational Frequencies (cm^{-1}).[a]

	All-Electron			ECP								Tentative
Exp.[b]	AE1	AE2	AE3	HS1	HS2	HS5	HS6	HS8	HS9	HS10	HS11	CC1	Assignment[c]
340	317	311	313	133	137	324	182	311	306	304	302	342	δ_s O—V—O
340	373	348	352	86	173	396	304	372	347	347	347	407	δ_{as} O—V—O
780	748	716	725	241	439	770	802	734	750	751	744	734	ν_{as} V—O
827[d]	826	798	806	296	355	798	1082	779	793	788	785	789	ν_s V—O

[a] Calculated frequencies are scaled by 0.9.
[b] From ref. 30.
[c] The assignment was based on the animation of the calculated vibrational modes carried out by Molecular Editor (ref. 31); ν = stretching; δ = bending; s = symmetric; as = antisymmetric.
[d] ν_s V—O = 820 cm^{-1} (ref. 11).

TABLE IV.
***Ab Initio* Fully Optimized Molecular Parameters for $(OH)VO_3^{2-}$ and $(OH)_3VO_2^{2-}$ Monovanadate Forms.[a]**

	All-Electron			ECP		
	AE1	AE2	AE3	HS5	HS8	CC1
$(OH)VO_3^{2-}$						
Bond lengths (pm)						
$V—O_1$	190	193	193	197	196	196
$V—O_{2,4}$	165	163	163	165	165	163
$V—O_3$	165	164	164	165	166	163
$O_1—H$	96	96	96	100	95	101
Bond angles (deg)						
$O_1—V—O_{2,4}$	107	108	108	107	108	107
$O_1—V—O_3$	102	104	103	106	102	109
$O_{2,3}—V—O_{3,4}$	113	112	112	112	113	112
$O_2—V—O_4$	113	112	112	113	113	111
$H—O_1—V$	107	106	106	107	107	109
Dihedral angle (deg)						
$H—O_1—V—O_3$	0	0	0	180	0	180
$(OH)_3VO_2^{2-}$						
Bond lengths (pm)						
$V—O_1$	192	194	194		196	
$V—O_2$	162	160	159		161	
$V—O_3$	196	199	198		196	
$V—O_4$	161	159	158		162	
$V—O_5$	199	201	201		205	
$O—H$	96	96	96		96	
Bond angles (deg)						
$O_1—V—O_2$	97	98	98		102	
$O_1—V—O_3$	79	79	79		79	
$O_1—V—O_4$	101	101	101		97	
$O_1—V—O_5$	153	159	159		154	
$O_3—V—O_4$	116	119	119		133	
$O_3—V—O_5$	77	80	80		77	
$O_4—V—O_5$	99	91	91		91	
$H—O—V$	105	103	103		108	
Dihedral angle (deg)						
$H_1—O_1—V—O_2$	142	137	136		105	
$H_1—O_1—V—O_3$	11	6	6		9	
$H_1—O_1—V—O_4$	−104	−111	−112		−142	
$H_1—O_1—V—O_5$	35	11	11		36	

[a] For the numbering of atoms, see Figure 1a and b.

ECP results, HS8 proves to be the only one to reproduce this result. With the two other ECPs (HS5 and CC1), it was found that the reproduction of the AE conformation with respect to the internal rotation about $HO_1—VO_3$ requires the inclusion of a diffuse function on the oxygen atoms. However, in addition to a large increase in CPU time, these additional basis functions lead to a much overestimated $H—O_1—V$ bond angle.

The possible occurrence of five-coordinate monovanadate ions in aqueous solutions has been discussed in the literature.[10] The calculated structure of the $(HO)_3VO_2^{2-}$ ion [resulting from the uptake of one molecule of water by $(HO)VO_3^{2-}$] is presented in Figure 1b and Table IV. Both all-electron and HS8 results predict a distorted trigonal-bipyramidal geometry, with a maximum O—V—O angle of ca. 160°. Considering the equilibrium

$$(HO)VO_3^{2-} + H_2O \Leftrightarrow (HO)_3VO_2^{2-}$$

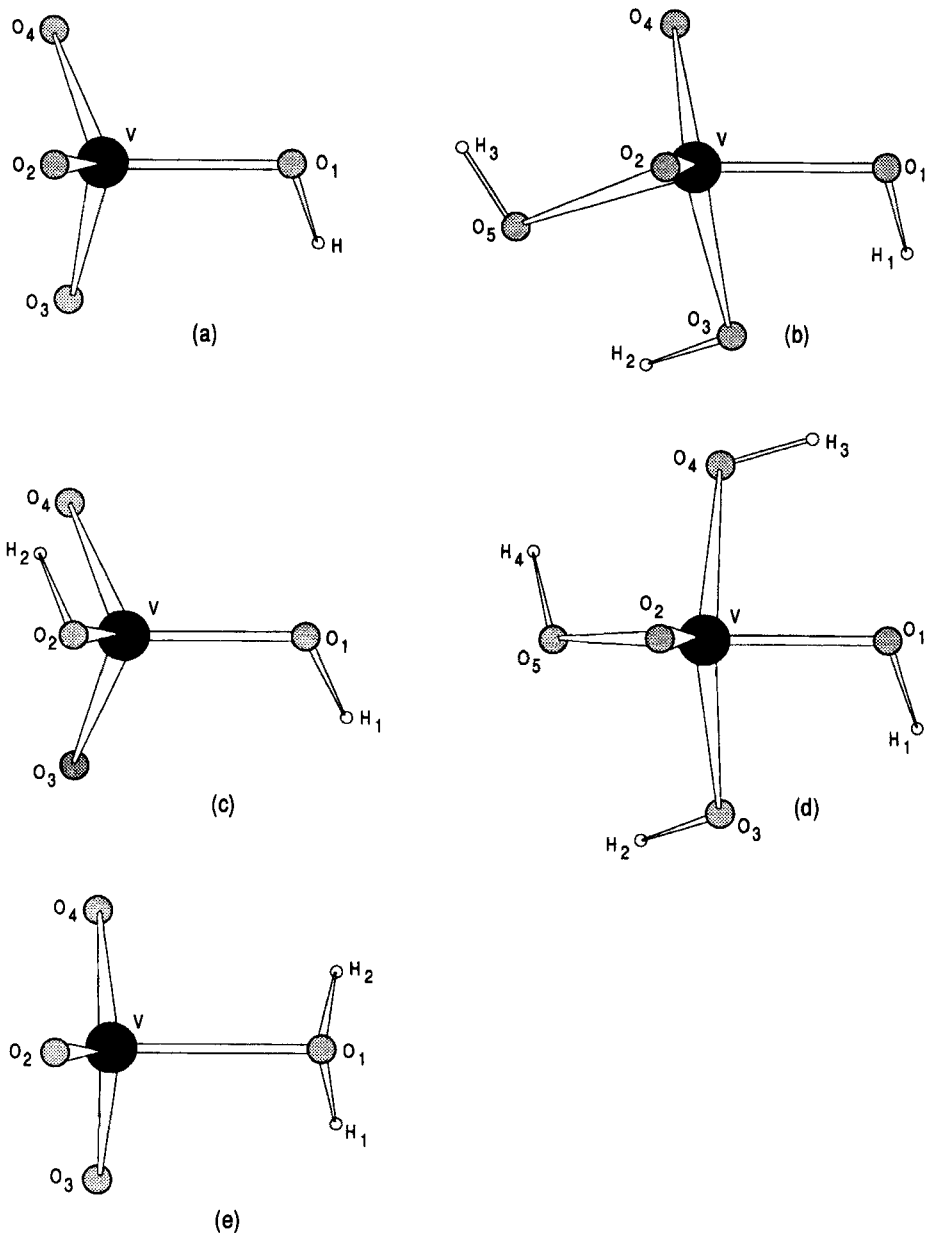

FIGURE 1. Optimized structures and numbering of the atoms for the monomeric species: (a) $(HO)VO_3^{2-}$, (b) $(HO)_3VO_2^{2-}$, (c) $(HO)_2VO_2^-$, (d) $(HO)_4VO^-$, and (e) $(H_2O)VO_3^-$.

the five-coordinate form is energetically favored by ca. 46 kJ mol^{-1} at the AE3 level and 75 kJ mol^{-1} at the HS8 level.

Table V shows the vibrational frequencies and their approximate descriptions[30,31] for these two monovanadate forms $[(HO)VO_3^{2-}$ and $(HO)_3VO_2^{2-}]$. The overall agreement between the HS8 and AE3 results for both species is good, despite some slight differences in frequency values. In particular, both approaches give relatively high values for the OV—OH torsional modes for the pentacoordinated form (387/414 and 516/538 cm^{-1}). On the other hand, it can be seen that for both HS8 and AE3, the ν_s V—O value of $(HO)VO_3^{2-}$ is more similar to the experimental values of the literature (see footnote b of Table V) than that calculated for the $(HO)_3VO_2^{2-}$ form. However, the difference in magnitude does not allow the assignment of the experimental value to a specific form.

Finally, with regard to HS5 and CC1, it was noticed that both ECPs tend to underestimate the

TABLE V.
$(OH)VO_3^{2-}$ and $(OH)_3VO_2^{2-}$ Monovanadate Forms Vibrational Frequencies (cm^{-1}).[a]

$(OH)VO_3^{2-}$			$(OH)_3VO_2^{2-}$		
AE3	HS8	Tentative Assignment[b]	AE3	HS8	Tentative Assignment[b]
113	126	τ OV—OH	57	70	δ O—V—O
245	232	δ O—V—O	171	213	τ OV—OH
256	248	δ O—V—O	234	230	δ O—V—O
327	337	δ O—V—O	291	279	δ O—V—O
356	355	δ O—V—O	312	303	δ O—V—O
363	365	δ O—V—O	320	321	δ O—V—O
521	492	ν V—O(H)	326	338	δ O—V—O
723	651	δ V—O—H	364	377	ν_{as} V—O(H)
890	884	ν_{as} V—O	370	378	δ O—V—O
893	900	ν V—O	387	414	τ OV—OH
927	903	ν_s V—O	444	462	ν_{as} V—O(H)
3623	3686	ν O—H	516	538	τ OV—OH
			527	545	ν_s V—O(H)
			778	771	δ V—O—H
			860	826	δ V—O—H
			869	863	δ V—O—H
			957	957	ν_s V—O2
			1007	966	ν_s V—O
			3623	3653	ν O—H
			3629	3677	ν_s (O—H)2
			3636	3681	ν_{as} (O—H)2

[a] Calculated frequencies are scaled by 0.9.
[b] The assignment was based on the animation of the calculated vibrational modes carried out by Molecular Editor (ref. 31); ν = stretching; δ = bending; τ = torsion; s = symmetric; as = antisymmetric. Experimental value of ν_s V—O is 877 cm^{-1} (ref. 30) and 870 cm^{-1} (ref. 11).

vibrational modes involving the hydrogen atoms and overestimate the V—O symmetric stretching frequency in $(HO)VO_3^{2-}$.

On considering the diprotonated species, the problem of locating the second hydrogen atom arises. Generally, it has been accepted that the structure of this species is $(HO)_2VO_2^-$. However, some authors suggested the possible alternative structure $(H_2O)VO_3^-$.[32] Both structures were found to be a minimum energy configuration in all the AE levels of calculation, the conventional $(HO)_2VO_2^-$ structure being more stable than $(H_2O)VO_3^-$ by ca. 200 kJ mol^{-1}. Among the three ECP levels tested, only HS8 yielded a minimum for the $(H_2O)VO_3^-$ structure, 180 kJ mol^{-1} above the $(HO)_2VO_2^-$ minimum.

A similar problem of hydrogen location has been discussed for the case of the five-coordinate form (general formulae $H_4VO_5^-$), considered to be the dominant form in aqueous solution.[10] However, for this form only the $(HO)_4VO^-$ structure was found to be a minimum, while the $(HO)_2(H_2O)VO_2^-$ structure splits in H_2O plus $(HO)_2VO_2^-$ during geometry optimization. The $(HO)_4VO^-$ form is energetically favored in the $H_2O + (HO)_2VO_2^- \Leftrightarrow (HO)_4VO^-$ equilibrium by ca. 6 and 15 kJ mol^{-1} at the AE3 and HS8 levels, respectively. As in the case of the monohydrogenvanadate, the small energy differences do not allow conclusions on the relative importance of the four- and five-coordinate forms in aqueous solution.

Table VI presents the calculated structural parameters for the *three forms of dihydrogenvanadate anion* and Figure 1c, d, and e shows the corresponding minimum energy structures obtained at the AE levels. As previously mentioned for the monoprotonated species, the lack of experimental data makes the AE calculations the real terms of comparison for the performances of the ECPs.

From Table VI, it can be concluded that the ECP calculated bond lengths and O—V—O bond angles are in good agreement with the corresponding AE results *in all forms*. On the other hand, the ECP H—O—V bond angle for $(HO)_2VO_2^-$ is largely overestimated, in particular at the HS8 level. Fi-

TABLE VI.
***Ab Initio* Fully Optimized Molecular Parameters for the Diprotonated Monovanadate Species in the $(OH)_2VO_2^-$, $(OH)_4VO^-$, and $(H_2O)VO_3^-$ Forms.[a]**

	All-Electron			ECP		
	AE1	AE2	AE3	HS5	HS8	CC1
$(HO)_2VO_2^-$						
Bond lengths (pm)						
$V—O_{1,2}$	182	183	183	182	182	182
$V—O_{3,4}$	159	157	157	160	160	158
$O_{1,2}—H_{1,2}$	96	96	96	97	95	97
Bond angles (deg)						
$O_1—V—O_2$	106	109	108	109	107	110
$O_{1,2}—V—O_{3,4}$	108	109	109	110	109	109
$O_{1,2}—V—O_{4,3}$	110	110	110	109	110	109
$O_3—V—O_4$	115	112	112	111	111	110
$H_{1,2}—O_{1,2}—V$	117	115	109	125	142	125
Dihedral angles (deg)						
$H_1—O_1—V—O_2$	105	102	102	96	110	97
$H_1—O_1—V—O_3$	−13	−17	−17	−24	−9	−22
$H_2—O_2—V—O_4$	−13	−17	−17	−24	−9	−22
$(HO)_4VO^-$						
Bond lengths (pm)						
$V—O_{1,3,4,5}$	185	186	186		186	
$V—O_2$	156	153	153		156	
$O—H$	96	96	100		96	
Bond angles (deg)						
$O_1—V—O_{3,4}$	85	85	85		85	
$O_1—V—O_5$	145	146	145		146	
$O_2—V—O_{1,3,4,5}$	107	107	107		107	
$H—O—V$	111	109	109		118	
Dihedral angles (deg)						
$H_1—O_1—V—O_2$	91	98	97		100	
$H_1—O_1—V—O_3$	−16	−9	−9		−7	
$(H_2O)VO_3^-$						
Bond lengths (pm)						
$V—O_1$	212	212	212		213	
$V—O_2$	160	160	160		162	
$V—O_{3,4}$	162	162	162		163	
$O_1—H_{1,2}$	97	97	97		96	
Bond angles (deg)						
$O_1—V—O_2$	110.2	110.8	110.2		108.5	
$O_1—V—O_{3,4}$	94.8	94.8	94.8		92.5	
$O_2—V—O_{4,3}$	117.2	117.1	117.2		118.0	
$O_3—V—O_4$	116.8	116.7	116.8		118.7	
$H_{1,2}—O_1—V$	98.7	98.7	98.6		110.4	
$H_1—O_1—H_2$	106.6	106.7	106.6		114.4	
Dihedral angles (deg)						
$H_1—O_1—V—O_2$	125.9	125.8	125.9		116.3	
$H_1—O_1—V—O_3$	4.6	4.5	4.6		−3.9	
$H_2—O_1—V—O_4$	1.8	−4.3	−4.4		4.7	

[a] For the numbering of atoms, see Figures 1c, d, and e, respectively.

nally, the AE values of the torsional angles are reasonably reproduced by the ECP levels. Comparing the two forms of $H_2VO_4^-$, the main differences arise in the V—O(H) bond lengths [larger in the case of V—O(H_2)] and O—V—O angles which, in the case of the $(H_2O)VO_3^-$ form, reflect a displacement of $O_{3,4}$ atoms toward the hydrogen atoms (see Fig. 1e). An interesting point is that both forms of $H_2VO_4^-$ present the same conformation for the OV—OH torsional angle. With regard to the $(HO)_4VO^-$ form, both all-electron and HS8 calculations yield a square-pyramidal structure, not far from the distorted trigonal-bipyramidal geometry found for $(HO)_3VO_2^{2-}$.

The calculated vibrational frequencies for the $(HO)_2VO_2^-$ and $(HO)_4VO^-$ forms are presented in Table VII. The overall agreement between the HS8 and the AE frequencies is acceptable for both forms, the largest differences being observed for the OH and antisymmetric V—O stretching modes. As previously found for the double charged forms, the ν_s V—O mode presents a higher value for the pentacoordinated form [$(HO)_4VO^-$].

In short, the previous results seem to elect HS8 as the best overall ECP calculation as it yields the best accuracy/computational cost ratio for the vanadate monomeric species herein considered. Its major limitations are restricted to the description of some molecular parameters related to the O—H bond in the protonated forms.

DIVANADATE SPECIES: $V_2O_7^{4-}$

On passing to the dimeric species, calculations were performed at the AE1 and the three previously selected ECP levels (HS5, HS8, and CC1) in

TABLE VII.
$(OH)_2VO_4^-$ and $(OH)_4VO^-$ Monovanadate Forms Vibrational Frequencies (cm^{-1}).[a]

$(OH)_2VO_4^-$			$(OH)_4VO^-$		
AE3	HS8	Tentative Assignment[b]	AE3	HS8	Tentative Assignment[b]
165	186	τ OV—OH	119	110	δ O—V—O
248	206	δ_{as} O—V—O	194	181	τ OV—OH
253	221	τ OV—OH	196	182	δ O—V—O
272	256	δ_{as} O—V—O	241	261	τ OV—OH
319	258	δ_s O—V—O	301	280	δ O—V—O
325	317	δ_{as} O—V—O	301	298	δ O—V—O
367	384	δ O—V—O	311	298	δ O—V—O
646	405	ν_{as} V—O	346	387	δ O—V—O
652	424	ν_{as} V—O	370	410	τ OV—OH
690	654	δ_{as} V—O—H	370	410	δ O—V—O
705	673	δ_s V—O—H	391	424	τ OV—OH
1027	1009	ν_{as} V—O	470	452	ν V—O
1048	1011	ν_s V—O	581	590	ν V—O
3623	3815	ν_{as} O—H	581	591	ν V—O
3623	3833	ν_s O—H	626	626	ν_s V—O
			807	703	δ V—O—H
			821	752	δ V—O—H
			821	752	δ V—O—H
			833	776	δ V—O—H
			1116	1074	ν_s V—O
			3632	3729	ν O—H
			3632	3730	ν O—H
			3633	3730	ν O—H
			3633	3731	ν O—H

[a] Calculated frequencies are scaled by 0.9.
[b] The assignment was based on the animation of the calculated vibrational modes carried out by Molecular Editor (ref. 31); ν = stretching; δ = bending; τ = torsion;; s = symmetric; as = antisymmetric.

TABLE VIII.
***Ab Initio* Fully Optimized Molecular Parameters for $V_2O_7^{4-}$.[a]**

	AE1	ECP			Exp.[b]
		HS5	HS8	CC1	
Bond lengths (pm)					
$V_1—O_1$	183	184	185	183	180
$V_1—O_2$	167	167	168	166	170
Bond angles (deg)					
$O_1—V_1—O_2$	110	110	110	111	105
$O_2—V_1—O_3$	109	109	109	108	113
$O_3—V_1—O_4$	109	109	109	108	113
$V_1—O_1—V_2$	180	180	180	180	141[c]
Dihedral angles (deg)					
$O_2—V_1—V_2—O_5$	180	180	180	180	
$O_2—V_1—V_2—O_6$	60	60	60	60	
$O_2—V_1—V_2—O_7$	−60	−60	−60	−60	

[a] For the numbering of atoms, see Figure 2.
[b] From X-ray results on $Mg_2V_2O_7$ (ref. 33).
[c] Other reported X-ray values are 149.3° (α-$Zn_2V_2O_7$) (ref. 34), 122.0° ($Pb_2V_2O_7$) and 124.0° (β-$Sr_2V_2O_7$) (ref. 35), 139° ($Ca_2V_2O_7$) (ref. 36), 180° ($Mn_2V_2O_7$, β-$Cu_2V_2O_7$, and $Cd_2V_2O_7$) (refs. 37–39).

order to assess the performances of these ECPs, in particular, for the evaluation of the V—O—V bond angle.

Table VIII shows the geometrical parameters calculated for $V_2O_7^{4-}$ using the AE1 basis set and the above-mentioned ECPs. Some previously reported X-ray results[33–39] of several salts are also included. Figure 2 shows the minimum energy structure obtained at the AE1 level.

The general agreement between the experimental and calculated V—O bond lengths is satisfactory, both at the AE and ECP levels. However, for the bond angles, both AE1 and the ECPs tend to overestimate the $O_1—V_m—O_n$ bond angles (m = 1, 2; n = 2–7) and underestimate the remaining O—V—O angles. A more decisive structural parameter is the V—O—V angle, as the question of the linearity of the $M_2O_7^{n-}$ species has raised some attention recently.[40] In the case of the $V_2O_7^{4-}$ anion, while the *ab initio* calculations herein reported are unanimous in pointing to a centrosymmetrical linear structure for the dimeric species, X-ray results yield both a linear or a bent geometry.[41]

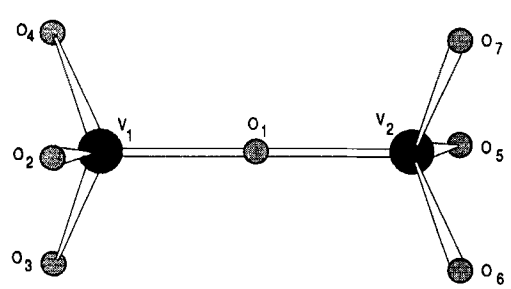

FIGURE 2. Optimized structure and numbering of the atoms for the dimeric ($V_2O_7^{4-}$) species.

Previous *ab initio* studies on siloxanes[42,43] conclude that the inclusion of a polarization function (*d*-type) on oxygen is required for the accurate calculation of the Si-O-Si angle. Being so, the disagreement *between some experimental* values (Table VIII) and the calculated results obtained in the present work does not seem to result from a basis set deficiency, at least of this kind. In fact, the AE1 basis set includes a polarization function on oxygen (see Experimental section). In addition, two tests were done at the HS8 level by adding a polarization function to the oxygen basis set (ζ = 0.8 and 0.7).[43] In both cases, a linear V—O—V bond was confirmed.

At this point, it is worth pointing out that the calculations were carried out for the isolated species, whereas the experimental data refer to solid-state samples. Hence, definite conclusions on the relative merits of the calculations are certainly difficult to reach by comparison with the experimental results. In particular, the experimental $V_1—O_1—V_2$ angle proves to be very sensitive to the type of cation in the salt, ranging from 180 to 124° (see Table VIII, footnotes b and c).

As mentioned before (see Experimental section), the single vibrational frequency calculation for this species was performed at the HS8 level (Table IX). While the calculated lower frequency modes are

TABLE IX.
$V_2O_7^{4-}$ Vibrational Frequencies (cm^{-1}).[a]

Exp. (ref. 30)	HS8	Tentative Assignment[b]
300	23	τ OV—VO
228	86	δ V—O_1—V
503	197	ν_s V—O_1
	209	δ (VO_3)
	327	δ (VO_3)
	358	δ (VO_3)
351	383	δ (VO_3)
	387	ν_{as} V—O_t
	461	ν_s V—O_t
810	687	ν_{as} V—O_1
	802	ν_{as} V—O_t
	822	ν_s V—O_t
850	851	ν_{as} V—O_t
877[c]	857	ν_s V—O_t

[a] For the numbering of atoms, see Figure 2. Calculated frequencies are scaled by 0.9.
[b] ν = stretching; δ = bending; τ = torsion; s = symmetric; as = antisymmetric; t = terminal.
[c] ν_s V—O_t = 870 cm^{-1} (ref. 11).

not consonant with previous empirical assignments,[30] a reasonable agreement is found for the higher frequency modes, especially if we keep in mind that the experimental results refer to a condensed phase. In particular, the present results support the assignment of the VO stretching mode of $V_2O_7^{4-}$ very close to the value for HVO_4^{2-} based on a simple bond order approach.[11]

NONCYCLIC TRIVANADATE AND TETRAVANADATE SPECIES: $V_3O_{10}^{5-}$ and $V_4O_{13}^{6-}$

Table X presents some molecular parameters obtained at the HS8 level for $V_3O_{10}^{5-}$ and $V_4O_{13}^{6-}$ (Fig. 3a and b, respectively). As mentioned above, no vibrational frequency calculations were performed for these vanadate species due to computational limitations. However, in the case of the trimeric species, single point calculations confirmed the herein reported geometry as an energy minimum at the HS8 level.

TABLE X.
***Ab Initio* Fully Optimized Molecular Parameters for $V_3O_{10}^{5-}$ and $V_4O_{13}^{6-}$.[a]**

	$V_3O_{10}^{5-}$				
		Exp.			
	Calc.	b	c	$V_4O_{13}^{6-}$	
Bond lengths (pm)					
V_1—O_1	180	180	177	V_1—O_1	180
V_2—O_1	189	188	181	V_1—O_6	180
				V_3—O_6	189
V_1—O_3	164	166	162	V_1—O_2	163
V_2—O_5	168	167	166	V_3—O_8	168
Bond angles (deg)					
O_1—V_1—O_2	117	110	111	O_1—V_1—O_6	118
O_1—V_1—O_3	108		111	O_1—V_1—O_2	107
O_1—V_2—O_5	110	112	109	O_2—V_1—O_6	108
O_3—V_1—O_4	108	107	114	O_6—V_3—O_8	110
O_5—V_2—O_6	109		109	O_2—V_1—O_3	109
O_6—V_2—O_7	109	108	114	O_8—V_3—O_9	109
				O_9—V_3—O_{10}	109
V_1—O_1—V_2	166	123	155	V_1—O_6—V_3	164
				V_1—O_1—V_2	180
Dihedral angles (deg)					
O_1—V_1—O_2—V_3	180	180	0	O_1—V_1—O_6—V_3	180
O_3—V_1—O_1—V_2	−60			O_2—V_1—O_6—V_3	−59
V_1—O_1—V_2—O_5	0	180	90	V_1—O_6—V_3—O_8	0
V_1—O_1—V_2—O_6	122			V_1—O_6—V_3—O_9	120
				V_2—O_1—V_1—O_6	86

[a] For numbering of atoms, see Figure 3a and b, respectively.
[b] X-ray results for $Na_5V_3O_{10} \cdot H_2O$ (ref. 44).
[c] X-ray results for $K_5V_3O_{10}$ (ref. 45).

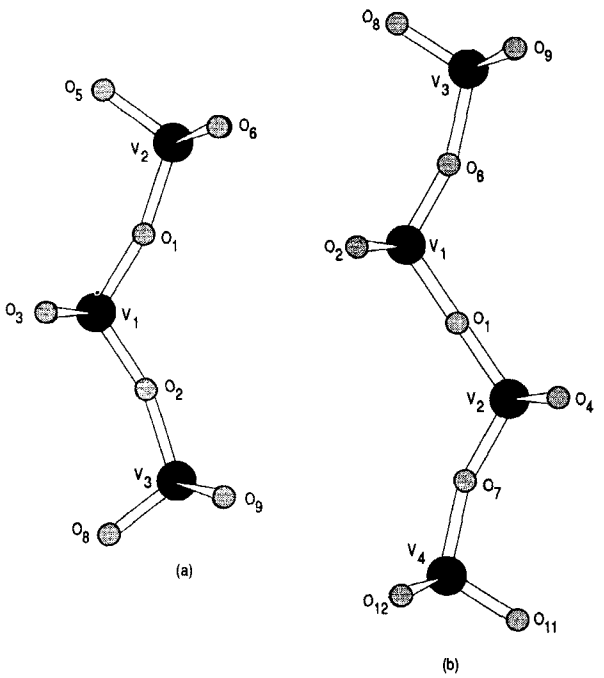

FIGURE 3. Optimized structures and numbering of the atoms for the linear (a) trivanadate ($V_3O_{10}^{5-}$) and tetravanadate ($V_4O_{13}^{6-}$) species. In (a), O_4, O_7, and O_{10} are eclipsed by O_3, O_6, and O_9, respectively. In (b), O_3, O_5, O_{10}, and O_{13} are eclipsed by O_2, O_4, O_9, and O_{12}, respectively.

Starting with the trimeric species (Fig. 3a), V—O_b bond lengths (e.g., V_1—O_1; "b" stands for bridging) are much longer than V—O_t (e.g., V_2—O_5; "t" stands for terminal). In addition, the central bridging V—O bond lengths (V_1—O_1 = V_1—O_2) are ca. 8 pm shorter than V_2—O_1 (or V_3—O_2). Similarly, the terminal V—O bond lengths at V_2 and V_3 (V_2—$O_{5,6,7}$ = V_3—$O_{8,9,10}$) are ca. 4 pm longe than those at the central vanadium atom (V_1—$O_{3,4}$).

With the exception of the central O_1—V_1—O_2 angle (117°), all the O—V—O angles are close to the tetrahedral angle (108–110°). The bond angles involving a bridging oxygen and a terminal vanadium atom (O_1—V_2—$O_{5,6,7}$ and O_2—V_3—$O_{8,9,10}$) are ca. 3° larger than those involing the central transition metal atom. However, the difference between the O—V—O angles involving two terminal oxygen atoms and the central or a terminal vanadium atom is smaller.

Finally, the V—O—V bond angle is considerably smaller than 180°. Hence, at the HS8 level, $V_3O_{10}^{5-}$ has a bent structure, in contrast to the dimeric species.

These calculated values are in general agreement with the X-ray molecular structures reported for this species,[44,45] namely, with regard to bond lengths and bond angles (see Table X). However, as in the case of the divanadate, the crystal structure of the linear trivanadate seems to be quite dependent on the nature of the salt. For instance, the V_1—O_1—V_2 angle is reported to be 123° in the potassium salt[45] and 155° in the sodium salt[44]; the latter is compared with the calculated value of 166°. Moreover, in the sodium salt each VO_4 tetrahedron is in a nearly eclipsed position with its neighbors, while in the potassium salt the two terminal VO_4 tetrahedra are oriented relative to each other halfway between eclipsed and staggered conformations. Not surprisingly, both cases are in disagreement with the calculated conformation for the isolated ion, which yields staggered relative orientation for adjacent VO_4 tetrahedra.

To the best of our knowledge, the molecular structures of the $V_4O_{13}^{6-}$ species have not been published to date. A single X-ray work reported the unit cell parameters of $Ba_3V_4O_{13}$ crystals.[46] As a result, the following discussion will be limited to the calculated molecular parameters.

The structural similarities between $V_4O_{13}^{6-}$ (Fig. 3b) and $V_3O_{10}^{5-}$ are quite clear. In fact, for $V_4O_{13}^{6-}$, V—O_b bonds are much longer than V—O_t, as was found for the trimeric species. Among V—O_t bond lengths, those involving central vanadium atoms are ca. 4 pm shorter than those which involve other vanadium atoms. In addition, V—O_b bond lengths involving the terminal vanadium atoms are also longer than those at the central vanadium atoms (ca. 5 and 9 pm longer than the $V_{1,2}$—O_1 and $V_{1,2}$—$O_{6,7}$, respectively).

In the same way, O—V—O bond angles have close values in the two noncyclic oligomeric species. The most remarkable difference arises for the O_b—V—O_b angles, which are ca. 2° larger in $V_4O_{13}^{6-}$ than in $V_3O_{10}^{5-}$.

As far as the V—O—V bond angles are concerned, the tetravanadate species show features of smaller oligomeric species, namely, $V_2O_7^{4-}$ and $V_3O_{10}^{5-}$. In fact, as for the trimeric species, the terminal V—O—V angles in $V_4O_{13}^{6-}$ are less than 180°, and the central angle ($V_1O_1V_2$) shows up as perfectly linear, in similarity to that on the dimeric species.

CYCLIC TETRAVANADATE SPECIES: $V_4O_{12}^{4-}$

Table XI presents some structural parameters obtained with the HS8 basis set for the cyclic

TABLE XI.
***Ab Initio* Fully Optimized Molecular Parameters for $V_4O_{12}^{4-}$.[a]**

	HS8	Exp.[b]
Bond lengths (pm)		
$V_1—O_1$	180	176.9 ± 0.8
$V_1—O_2$	162	165
Bond angles (deg)		
$O_1—V_1—O_2$	111	111
$O_2—V_1—O_3$	109	102
$O_1—V_1—O_6$	106	112
$V_1—O_1—V_2$	164	158
Dihedral angles (deg)		
$O_1—V_1—O_6—V_3$	0	0
$O_2—V_1—O_1—V_2$	120	

[a] For the numbering of atoms, see Figure 4.
[b] X-ray results for $[(CH_3)_3CNH_3]_4[V_4O_{12}]$ (ref. 47).

tetravanadate species. Some X-ray results from the literature are also included. The corresponding molecular geometry is schematically represented in Figure 4.

As can be seen, the HS8 calculation yields a $V_4O_{12}^{4-}$ geometry with the four vanadium and the four bridging oxygens forming two different squares, each one rotated by 45° with respect to the other, yielding a strictly planar V_4O_4 ring. The terminal oxygen atoms lay above and below this ring. The resulting structure is in agreement with the X-ray results of Román et al.[47]

The overall agreement between our HS8 molecular parameters and the X-ray corresponding results[47] is quite reasonable. The differences between the calculated and experimental values do not exceed 3 pm for the V—O bond lengths and 7° for the bond angles. Once again, the observed discrepancies may result from different study conditions, namely, isolated molecule for the calculations versus crystal of $[(CH_3)CNH_3][V_4O_{12}]$ salt for the X-ray experiments.

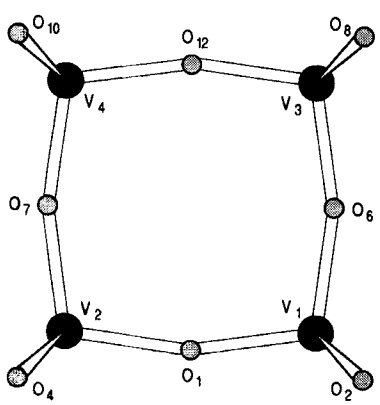

FIGURE 4. Optimized structure and numbering of the atoms for the cyclic tetravanadate ($V_4O_{12}^{4-}$) species. O_3, O_5, O_9, and O_{11} are eclipsed by O_2, O_4, O_8, and O_{10}, respectively.

As found for the other oligomeric species so far studied, V—O_b bonds are longer than V—O_t bonds. In addition, the V—O—V bond angles are bent, displaying the same values as in the noncyclic tri- and tetravanadate species. However, probably due to the constraints imposed by cyclization, the O—V—O angles are all within a range which is narrower for the cyclic species than for the noncyclic species.

A question usually raised about the tetravanadate species is the relative stability of the linear and cyclic forms. Considering the cyclization equilibrium

$$V_4O_{13}^{6-} + 2H_3O^+ \Leftrightarrow V_4O_{12}^{4-} + 3H_2O$$

the species on the right-hand side are more stable than those on the left-hand side by ca. 3.7×10^3 kJ mol^{-1} at the HS8 level. While this ΔE value cannot be directly related with a ΔG or ΔH value for the equilibrium in aqueous solution, it clearly supports the higher stability of the cyclic form of tetravanadate.

The crystal structure of the protonated cyclic tetramer was found to be nonplanar.[48] In order to provide some information as to the structural changes promoted by the protonation, a test was performed for $HV_4O_{12}^{3-}$, with the experimental geometry (symmetry of the ring nearly D_{2d}).[48] The optimized geometry is nearly planar, with the V(O) and V(OH) atoms deviated from the plane defined by the ring oxygen atoms by only ca. 10 and 30 pm, respectively. The V—O—V bond angles involving the V(OH) atom are smaller than the others by ca. 7°, while in the crystal structure they are 14° larger. On the other hand, the V—O(H) bond length is ca. 20 pm longer than the other terminal V—O bond lengths, in excellent agreement with the experimental values.[48]

Acknowledgments

The authors thank the referees for their helpful suggestions.

References

1. H. Degani, M. Gochin, S. J. D. Karlish, and Y. Shechter, *Biochemistry*, **20**, 5795 (1981).

2. J. Meyerovitch, Z. Farfel, J. Sack, and Y. Shechter, *J. Biol. Chem.*, **262,** 6658 (1987).
3. Y. Shechter, A. Shisheva, R. Lazar, J. Libman, and A. Shanzer, *Biochemistry*, **31,** 2063 (1992).
4. N. D. Chasteen, *Structure and Bonding*, **53,** 105 (1983).
5. D. C. Crans and P. K. Shin, *Inorg. Chem.*, **27,** 1797 (1988).
6. (a) M. Aureliano and V. M. C. Madeira, *Biochem. Biophys. Acta*, **1221,** 259 (1994); (b) D. Rehder, *Angew. Chem. Int. Ed. Engl.* **30,** 148 (1991); (c) V. I. Vashchenko, R. S. Utegalieva, and O. V. Esyrev, *Biochem. Biophys. Acta*, **1079,** 8 (1991); (d) D. C. Crans and C. M. Simone, *Biochemistry*, **30,** 6734 (1991); (e) D. C. Crans, E. M. Willging, and S. R. Butler, *J. Am. Chem. Soc.*, **112,** 427 (1990); (f) D. C. Crans and S. M. Schelble, *Biochemistry*, **29,** 6698 (1990); N. D. Chasteen, *Structure and Bonding*, **53,** 105 (1992) and references therein.
7. J. A. Connor, I. H. Hillier, V. R. Saunders, M. H. Wood, and M. Barber, *Mol. Phys.*, **24,** 497 (1972).
8. J.-Y. Kempf, M.-M. Rohmer, J.-M. Poblet, C. Bo, and M. Bérnard, *J. Am. Chem. Soc.*, **114,** 1136 (1992).
9. (a) M. Krauss and H. Basch, *J. Am. Chem. Soc.*, **114,** 3630 (1992); (b) M.-M. Rohmer and M. Bérnard, *J. Am. Chem. Soc.*, **116,** 6959 (1994).
10. S. E. Harnung, E. Larsen, and E. J. Pedersen, *Acta Chim. Scand.*, **47,** 674 (1993).
11. A. M. Amado, M. Aureliano, P. J. A. Ribeiro-Claro, and J. J. C. Teixeira-Dias, *J. Raman Spectrosc.*, **24,** 699 (1993).
12. M. J. Frisch, G. W. Trucks, M. Head-Gordon, P. M. W. Gill, M. W. Wong, J. B. Foresman, B. G. Johnson, H. B. Schlegel, M. A. Robb, E. S. Reploge, R. Gomperts, J. L. Andres, K. Raghavachari, J. S. Binkley, C. Gonzalez, R. L. Martin, D. J. Fox, D. J. DeFrees, J. Baker, J. J. P. Stuart, and J. A. Pople, GAUSSIAN 92, Revision C, Pittsburgh, 1992.
13. P. J. Hay and W. R. Wadt, *J. Chem. Phys.*, **82,** 270 (1985).
14. P. J. Hay and W. R. Wadt, *J. Chem. Phys.*, **82,** 299 (1985).
15. W. J. Stevens, H. Basel, and M. Krauss, *J. Chem. Phys.*, **81,** 6026 (1984).
16. V. Jonas, G. Frencking, and M. T. Reetz, *J. Comp. Chem.*, **13,** 919 (1992).
17. M. M. Hurley, L. F. Pacios, P. A. Christiansen, R. B. Ross, and W. C. Ermler, *J. Chem. Phys.*, **84,** 6840 (1986).
18. L. F. Pacios and P. A. Christiansen, *J. Chem. Phys.*, **82,** 2664 (1985).
19. T. Clark, J. Chandrasekhar, G. W. Spitznagel, and R. v. R. Schleyer, *J. Comp. Chem.*, **4,** 294 (1983).
20. W. J. Hehre, L. Radom, R. v. R. Schleyer, and J. A. Pople, *Ab Initio Molecular Orbital Theory*, John Wiley & Sons, New York, 1986, p. 82.
21. J. S. Binkley, J. A. Pople, and W. J. Hehre, *J. Am. Chem. Soc.*, **102,** 939 (1980).
22. K. D. Dobbs and W. J. Hehre, *J. Comp. Chem.*, **8,** 861 (1987).
23. P. Politzer and R. S. Mulliken, *J. Chem. Phys.*, **55,** 5135 (1971).
24. R. Gopal and C. Calvo, *Can J. Chem.*, **49,** 3056 (1971).
25. F. D. Hartcastle and I. E. Wachs, *J. Phys. Chem.*, **95,** 5031 (1991).
26. A. Veldkamp and G. Frenking, *J. Comp. Chem.*, **13,** 1184 (1992).
27. R. Stegmann, A. Neuhaus, and G. Frenking, *J. Am. Chem. Soc.*, **115,** 11930 (1993).
28. A. W. Ehlers and G. Frenking, *J. Am. Chem. Soc.*, **116,** 1514 (1994).
29. A. Veldkamp and G. Frenking, *J. Am. Chem. Soc.*, **116,** 4937 (1994).
30. W. Griffith and T. D. Wickins, *J. Chem. Soc. A*, 1087 (1966).
31. R. Wargo and A. Smith, *Molecular Editor, Version 1.1*, Drexel University, 1986.
32. O. W. Howarth, *Prog. NMR Spectrosc.*, **22,** 453 (1990).
33. R. Gopal and C. Calvo, *Acta Crystallogr., Sect. B*, **30,** 2491 (1974).
34. R. Gopal and C. Calvo, *Can J. Chem.*, **51,** 1004 (1973).
35. R. D. Shannon and C. Calvo, *CAn J. Chem.*, **51,** 70 (1973).
36. M. T. Pope, *Comprehensive Coordination Chemistry. The Synthesis, Reactions, Properties, & Applications of Coordination Compounds*, Pergamon Press, New York, 1987, p. 1023.
37. E. Doem and B.-O. Marinder, *Acta Chem. Scand.*, **21,** 590 (1967).
38. P. K. L. Au and C. Calvo, *Can. J. Chem.*, **45,** 2297 (1967).
39. D. Mercurio-Lavaud and B. Frit, *C. R. Acad. Sci. Paris C. Chim.*, **277,** 1101 (1973).
40. P. Kiprof, W. A. Herrmann, F. E. Kühn, W. Scherer, M. Kleine, M. Elison, and K. Rypdal, *Bull. Soc. Chim. Fr.*, **129,** 655 (1992).
41. G. M. Clark and R. Morley, *Chem. Soc. Rev.*, **5,** 269 (1976).
42. C. W. Earley, *J. Comp. Chem.*, **14,** 216 (1993).
43. S. Grigorás and T. H. Lane, *J. Comp. Chem.*, **8,** 84 (1987).
44. K. Kato and E. Takayama-Muromachi, *Acta Crystallogr., Sect. C*, **41,** 1409 (1985).
45. K. Kato and E. Takayama-Muromachi, *Acta Crystallogr., Sect. C*, **41,** 647 (1985).
46. J. M. Millet, H. S. Parker, and R. S. Roth, *J. Am. Ceram. Soc.*, **69,** C-103 (1986).
47. P. Román, A. S. José, A. Luque, and J. M. Guitérrez-Zorrilla, *Inorg. Chem.*, **32,** 775 (1993).
48. J. Fuchs, S. Mahjour, and J. Pickardt, *Angew. Chem. Int. Ed. Engl.*, **15,** 374 (1976).